IEEE Access
Multidisciplinary | Rapid Review | Open Access Journal

Received January 17, 2019, accepted February 10, 2019, date of publication February 15, 2019, date of current version March 5, 2019.

Digital Object Identifier 10.1109/ACCESS.2019.2899587

Feedback-Added Pseudoinverse-Type Balanced Minimization Scheme for Kinematic Control of Redundant Robot Manipulators

ZHENHUAN WANG[1], BOYANG WANG[2], LINGJIE XU[2], AND QINYU XIE[2]
[1]Space Control and Inertial Technology Research Center, Harbin Institute of Technology, Harbin 150001, China
[2]Department of Control Science and Engineering, School of Astronautics, Harbin Institute of Technology, Harbin 150001, China

Corresponding author: Zhenhuan Wang (zhenhuanwang@hit.edu.cn)

This work was supported in part by the National Natural Science Foundation of China under Grant 61703123, Grant 61640301, Grant 61673130, and Grant 61703120, and in part by the Self-Planned Task of the State Key Laboratory of Robotics and System (Harbin Institute of. Technology) under Grant SKLRS201806B.

ABSTRACT In this paper, a new feedback-added pseudoinverse-type balanced minimization (FPBM) scheme is proposed and studied for the kinematic control of redundant robot manipulators. Such a scheme is designed by combining the minimum acceleration norm (MAN) solution and the weighted minimum velocity norm (WMVN) solution and by introducing the feedback. With the MAN and WMVN combination, the proposed FPBM scheme can not only remedy the phenomena of high velocity and acceleration but also generate a near-zero velocity after task execution. With the feedback introduction, the proposed FPBM scheme can guarantee a nondivergent end-effector tracking error. Based on a four-link robot manipulator, the simulation results are presented to show the effectiveness of the proposed FPBM scheme.

INDEX TERMS Balanced minimization, pseudoinverse, feedback, kinematic control, redundant robot manipulators.

I. INTRODUCTION

Redundant robot manipulators are playing a significant role in many science and engineering fields [1]–[13]. The redundancy-resolution problem is one important issue in the kinematic control of redundant robot manipulators [1]–[6], [14]–[24]. This problem is generally described as: given the end-effector desired path, the corresponding joint solution need to be determined in real time. The classical solution to the redundancy-resolution problem is the pseudoinverse-type technique. This technique is a powerful alternative for the kinematic control of redundant robot manipulators. By exploiting the pseudoinverse-type technique, many studies have been reported on redundant robot manipulators [14], [15], [17], [19], [21]–[27].

As one special pseudoinverse-type scheme at the joint velocity level, the minimum velocity norm (MVN) scheme is widely adopted to the kinematic control of redundant robot manipulators [1], [2], [14], [15], [24]. In addition, a common variation of this minimum norm scheme is the weighted scheme that minimizes a weighted two norm (e.g., the weighted MVN scheme) [1], [2], [14], [15], [21]. Being another typical pseudoinverse-type scheme at the joint acceleration level, the minimum acceleration norm (MAN) scheme is also widely employed for the kinematic control of redundant robot manipulators [21]. However, there exist some drawbacks/limitations in the velocity level and acceleration level schemes.

On the one hand, the weighted MVN (WMVN) scheme (as a velocity level scheme) can only be applicable for the robot manipulators controlled by joint velocity. Due to the lack of information of joint acceleration and joint torque, the WMVN scheme can not be directly applied to the acceleration-controlled or torque-controlled robot manipulators. In this sense, the application field of the WMVN scheme is considerably limited [5], [21]. On the other hand, the MAN scheme (as an acceleration level scheme) can be applicable for the velocity-, acceleration-, or torque-controlled robot manipulators, thereby being advantageous over the WMVN scheme. However, the MAN scheme may not necessarily minimize the magnitudes of the individual joint acceleration, which would lead to a (relatively) high velocity or acceleration for a particular joint [14], [15], [28]–[31]. In addition, this scheme

The associate editor coordinating the review of this manuscript and approving it for publication was Min Wang.

would generate a non-zero final velocity that less desirable in applications. Evidently, there exist inherent issues for the WMVN and MAN schemes. It is thus necessary to develop an effective scheme to conquer the aforementioned problems.

In this paper, to avoid the limited application field and to remedy the phenomena of high-velocity/acceleration and non-zero final velocity, a new feedback-added pseudoinverse-type balanced minimization (FPBM) scheme is proposed and studied. Specifically, by combining the WMVN and MAN solutions via a weighting factor and by introducing the feedback, the FPBM scheme is developed for the kinematic control of redundant robot manipulators. This is the first time to provide a pseudoinverse-type scheme with the WMVN and MAN combination. Because of the feedback introduction, a prominent advantage of the proposed scheme is that the scheme can guarantee an end-effector tracking error with no divergence. Simulation results based on a four-link robot manipulator [21] are presented to further verify the effectiveness of the proposed FPBM scheme.

The rest of this paper is organized into four sections. Section II presents the preliminaries about the WMVN and MAN schemes. Section III describes the detailed formulation of the proposed FPBM scheme, together with the scheme derivation. Section IV shows the simulation results that are synthesized by the proposed FPBM scheme. Section V concludes this paper with final remarks.

II. PRELIMINARIES

In this section, some preliminaries about the pseudoinverse-type technique to the kinematic control of redundant robot manipulators are presented. In addition, the formulations of the WMVN and MAN schemes are given to lay a basis for further discussion.

A. ROBOTIC REDUNDANCY RESOLUTION

The redundancy resolution problem is a fundamental issue that corresponds to the kinematic control of redundant robot manipulators [1], [2], [5], [14], [15], [21], [24]. Mathematically, solving this problem can be equivalent to the solution to the following kinematic system:

$$f(q(t)) = x(t), \tag{1}$$

where $q(t) \in R^n$ is the joint angle vector, $x(t) \in R^m$ is the end-effector desired path, and $f(\cdot)$ is the differentiable nonlinear mapping. Note that $n > m$ in (1). This means that, given $x(t)$, an infinite number of $q(t)$ are possible.

By differentiating (1) with respect to time t, the redundancy resolution of robot manipulators can be studied at the joint-velocity level:

$$J(q)\dot{q} = \dot{x}, \tag{2}$$

where $J(q) \in R^{m\times n}$ is the Jacobian matrix, $\dot{q} \in R^n$ is the joint velocity vector, and $\dot{x} \in R^m$ is the time derivative of x. Based on (2), the pseudoinverse-type technique at the joint-velocity level is written as follows [1], [2], [21]:

$$\dot{q} = J^+\dot{x} + (I - J^+J)c, \tag{3}$$

where $J^+ \in R^{m\times n}$ is the pseudoinverse of J, $I \in R^{n\times n}$ is the identity matrix, and $c \in R^n$ is the vector selected by some optimization criteria. Different selections of c in (3) result in different pseudoinverse-type schemes for the kinematic control of redundant robot manipulators at the joint-velocity level.

By differentiating (2) with respect to time t, the redundancy resolution of robot manipulators can be further studied at the joint-acceleration level:

$$J\ddot{q} = \ddot{x} - \dot{J}\dot{q}, \tag{4}$$

where $\ddot{q} \in R^n$ is the joint acceleration vector, and $\ddot{x}$ and $\dot{J}$ are the time derivatives of $\dot{x}$ and J, respectively. Based on (4), the pseudoinverse-type technique at the joint-acceleration level is written as follows [1], [2], [21]:

$$\ddot{q} = J^+(\ddot{x} - \dot{J}\dot{q}) + (I - J^+J)c. \tag{5}$$

Similarly, selecting different c leads to different pseudoinverse-type schemes for the kinematic control of redundant robot manipulators at the joint-acceleration level.

On the basis of the above formulations, the pseudoinverse-type technique is depicted in an analytical-solution form, and it can thus solve the redundancy resolution problem readily. This significant characteristic has popularized the research and application of the pseudoinverse-type technique in the past decades [1], [2], [14], [15], [17], [19], [21]–[23], [32]–[36].

B. WMVN AND MAN SCHEMES

Being a special velocity level scheme, the pseudoinverse-type MVN scheme is widely adopted to redundant robot manipulators. This scheme is derived from (3) with $c = 0$ and is given as follows [1], [2], [14], [15]:

$$\dot{q} = J^+\dot{x}. \tag{6}$$

As a common variation of the MVN scheme (6), the WMVN scheme is formulated as follows:

$$\dot{q} = J_W^+\dot{x} = W^{-1}J^T(JW^{-1}J^T)^{-1}\dot{x}, \tag{7}$$

where $W \in R^{n\times n}$ is a positive definite matrix. Evidently, (7) reduces to (6) when $W = I$. This means that the WMVN scheme (7) is considered as a generalized form of the MVN scheme (6) for the kinematic control of redundant robot manipulators. In addition, the solution of $\dot{q}$ computed by the WMVN scheme (7) is the solution to the following minimization problem:

$$\min \{\dot{q}^T W \dot{q}\} \quad \text{subject to } J\dot{q} = \dot{x}.$$

where the superscript "T" is the transpose operator.

Being a typical acceleration level scheme, the pseudoinverse-type MAN scheme is also widely employed for redundant robot manipulators. This scheme is derived from (5) with $c = 0$ and is presented as follows [1], [2], [21]:

$$\ddot{q} = J^+(\ddot{x} - \dot{J}\dot{q}). \tag{8}$$

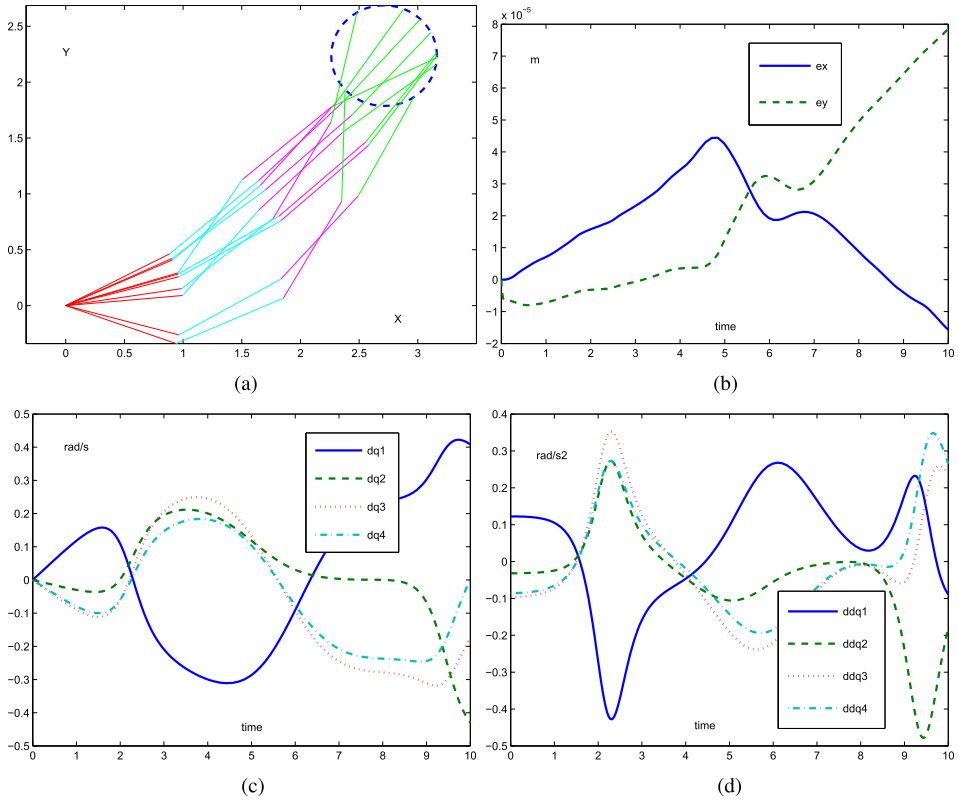

FIGURE 1. The four-link robot manipulator tracks a circular path by using the MAN scheme (8). (a) Motion trajectories. (b) End-effector tracking errors. (c) Profiles of joint velocity $\dot{q}$. (d) Profiles of joint acceleration $\ddot{q}$.

The solution computed by the MAN scheme (8) is the solution to the following minimization problem:

$$\min \{\ddot{q}^{\mathrm{T}}\ddot{q}\} \quad \text{subject to } J\ddot{q} = \ddot{x} - \dot{J}\dot{q}.$$

III. NEW FPBM SCHEME

In this section, based on the WMVN scheme (7) and the MAN scheme (8), the new FPBM scheme is proposed for the kinematic control of redundant robot manipulators.

For further discussion, the following lemmas are presented.

Lemma 1: The time derivative of J_{W}^{+} is formulated as follows:

$$\dot{J}_{\mathrm{W}}^{+} \triangleq \frac{\mathrm{d}J_{\mathrm{W}}^{+}}{\mathrm{d}t} = (I - J_{\mathrm{W}}^{+}J)W^{-1}\dot{J}^{\mathrm{T}}(JW^{-1}J^{\mathrm{T}})^{-1} - J_{\mathrm{W}}^{+}\dot{J}J_{\mathrm{W}}^{+}.$$

Proof: Given that $J_{\mathrm{W}}^{+} = W^{-1}J^{\mathrm{T}}(JW^{-1}J^{\mathrm{T}})^{-1}$, we have the following time derivative:

$$\begin{aligned}\dot{J}_{\mathrm{W}}^{+} \triangleq \frac{\mathrm{d}J_{\mathrm{W}}^{+}}{\mathrm{d}t} &= W^{-1}\frac{\mathrm{d}(J^{\mathrm{T}})}{\mathrm{d}t}(JW^{-1}J^{\mathrm{T}})^{-1} \\ &\quad + W^{-1}J^{\mathrm{T}}\frac{\mathrm{d}((JW^{-1}J^{\mathrm{T}})^{-1})}{\mathrm{d}t} \\ &= W^{-1}\dot{J}^{\mathrm{T}}(JW^{-1}J^{\mathrm{T}})^{-1} - J_{\mathrm{W}}^{+}JW^{-1} \\ &\quad \times \dot{J}^{\mathrm{T}}(JW^{-1}J^{\mathrm{T}})^{-1} - J_{\mathrm{W}}^{+}\dot{J}J_{\mathrm{W}}^{+} \\ &= (I - J_{\mathrm{W}}^{+}J)W^{-1}\dot{J}^{\mathrm{T}}(JW^{-1}J^{\mathrm{T}})^{-1} - J_{\mathrm{W}}^{+}\dot{J}J_{\mathrm{W}}^{+}.\end{aligned}$$

The proof is thus completed. □

Lemma 2: The matrix J_{W}^{+} satisfies the following properties:

$$(I - J_{\mathrm{W}}^{+}J)J_{\mathrm{W}}^{+} = 0, (I - J^{+}J)J_{\mathrm{W}}^{+} = J_{\mathrm{W}}^{+} - J^{+},$$
$$(I - J_{\mathrm{W}}^{+}J)(I - J_{\mathrm{W}}^{+}J) = (I - J^{+}J)(I - J_{\mathrm{W}}^{+}J) = I - J_{\mathrm{W}}^{+}J.$$

Proof: It can be generalized from $JJ_{\mathrm{W}}^{+} = I \in R^{m\times m}$. □

For the WMVN scheme (7) and the MAN scheme (8), their decision variables are different from each other; that is, the former is the joint velocity $\dot{q}$ and the latter is the joint acceleration $\ddot{q}$. To combine the WMVN and MAN solutions, the WMVN scheme (7) needs to be extended to the acceleration level one for redundant robot manipulators.

Theorem 1: The WMVN scheme (7) is equivalent to the acceleration level scheme as follows:

$$\ddot{q} = J_{\mathrm{W}}^{+}(\ddot{x} - \dot{J}\dot{q}) + (I - J_{\mathrm{W}}^{+}J)W^{-1}\dot{J}^{\mathrm{T}}(JW^{-1}J^{\mathrm{T}})^{-1}\dot{x}. \tag{9}$$

Proof: Given that $JJ_{\mathrm{W}}^{+} = I \in R^{m\times m}$, similar to the WMVN scheme (7), the following weighted scheme at the joint acceleration level can be derived:

$$\ddot{q} = J_{\mathrm{W}}^{+}(\ddot{x} - \dot{J}\dot{q}) + (I - J_{\mathrm{W}}^{+}J)c. \tag{10}$$

To develop an acceleration level scheme with the WMVN characteristic, c should be selected via the WMVN criterion.

Differentiating (7) with respect to time t, the following result is obtained:

$$\ddot{q} = J_{\mathrm{W}}^{+}\ddot{x} + \dot{J}_{\mathrm{W}}^{+}\dot{x}. \tag{11}$$

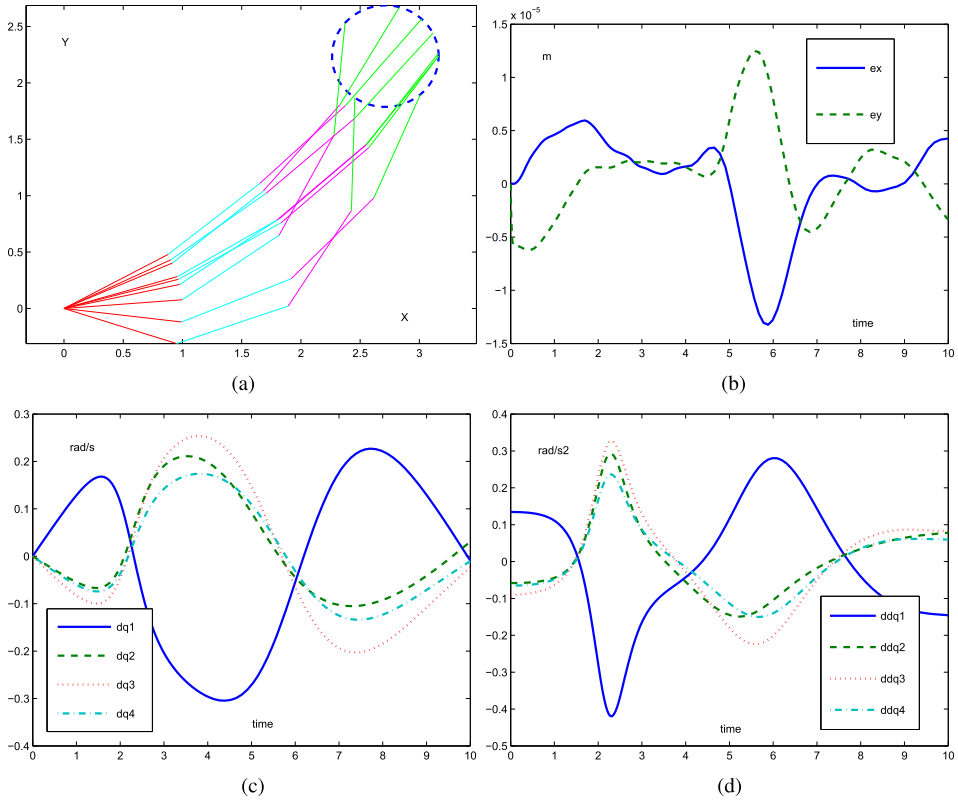

FIGURE 2. The four-link robot manipulator tracks a circular path by using the proposed FPBM scheme (13) with $\alpha = 0.6$, $k_1 = k_2 = 1$ and $W = \text{diag}\{1, 2, 3, 4\}$. (a) Motion trajectories. (b) End-effector tracking errors. (c) Profiles of joint velocity $\dot{q}$. (d) Profiles of joint acceleration $\ddot{q}$.

By replacing c with (11), the acceleration level scheme derived from (10) is presented as follows:

$$\ddot{q} = J_{\mathrm{W}}^{+}(\ddot{x} - \dot{J}\dot{q}) + (I - J_{\mathrm{W}}^{+}J)(J_{\mathrm{W}}^{+}\ddot{x} + \dot{J}_{\mathrm{W}}^{+}\dot{x}). \tag{12}$$

Based on the results in Lemmas 1 and 2, the acceleration level scheme (12) is reformulated as follows:

$$\ddot{q} = J_{\mathrm{W}}^{+}(\ddot{x} - \dot{J}\dot{q}) + (I - J_{\mathrm{W}}^{+}J)W^{-1}\dot{J}^{\mathrm{T}}(JW^{-1}J^{\mathrm{T}})^{-1}\dot{x}.$$

which is exactly (9) with the WMVN characteristic. By summarizing the above analysis, the WMVN scheme (7) processes the equivalence to the acceleration level scheme (9). The proof is thus completed. □

On the basis of Theorem 1, the following FPBM scheme based on the combination of WMVN and MAN schemes is thus developed for the kinematic control of redundant robot manipulators.

Theorem 2: The FPBM scheme proposed in this paper is formulated as

$$\begin{aligned}\ddot{q}_{(\mathrm{FPBM})} = {} & (\alpha J_{\mathrm{W}}^{+} + (1-\alpha)J^{+})(\ddot{x} - \dot{J}\dot{q} + k_1(\dot{x} - J\dot{q}) \\ & + k_2(x - f(q))) + \alpha(I - J_{\mathrm{W}}^{+}J)W^{-1} \\ & \times \dot{J}^{\mathrm{T}}(JW^{-1}J^{\mathrm{T}})^{-1}\dot{x},\end{aligned} \tag{13}$$

where $\alpha \in [0, 1]$ is the weighting factor, and $k_1 > 0 \in R$ and $k_2 > 0 \in R$ are the feedback gains.

Proof: Recall the pseudoinverse-type technique (5), i.e.,

$$\ddot{q} = J^{+}(\ddot{x} - \dot{J}\dot{q}) + (I - J^{+}J)c.$$

By employing a weighting factor α and replacing c with (9), the following result is derived:

$$\ddot{q} = J^{+}(\ddot{x} - \dot{J}\dot{q}) + \alpha(I - J^{+}J)\ddot{q}_{(\mathrm{WMVN})}, \tag{14}$$

where $\ddot{q}_{(\mathrm{WMVN})}$ is obtained by (9). Based on the results in Lemma 2 and Theorem 1, (14) is transformed as follows:

$$\ddot{q} = (1 - \alpha)\ddot{q}_{(\mathrm{MAN})} + \alpha\ddot{q}_{(\mathrm{WMVN})}, \tag{15}$$

where $\ddot{q}_{(\mathrm{MAN})}$ is obtained by (8). Therefore, by substituting (8) and (9) into (15), we have

$$\begin{aligned}\ddot{q} &= (1 - \alpha)\ddot{q}_{(\mathrm{MAN})} + \alpha\ddot{q}_{(\mathrm{WMVN})}, \\ &= (\alpha J_{\mathrm{W}}^{+} + (1-\alpha)J^{+})(\ddot{x} - \dot{J}\dot{q}) + \alpha(I - J_{\mathrm{W}}^{+}J)W^{-1} \\ &\quad \times \dot{J}^{\mathrm{T}}(JW^{-1}J^{\mathrm{T}})^{-1}\dot{x}.\end{aligned} \tag{16}$$

For (16), it would generate a divergence end-effector tracking error. To overcome this issue, by introducing the feedback based on (1) and (2), the following result is obtained:

$$\begin{aligned}\ddot{q}_{(\mathrm{FPBM})} = {} & (\alpha J_{\mathrm{W}}^{+} + (1-\alpha)J^{+})(\ddot{x} - \dot{J}\dot{q} + k_1(\dot{x} - J\dot{q}) \\ & + k_2(x - f(q))) + \alpha(I - J_{\mathrm{W}}^{+}J)W^{-1} \\ & \times \dot{J}^{\mathrm{T}}(JW^{-1}J^{\mathrm{T}})^{-1}\dot{x},\end{aligned}$$

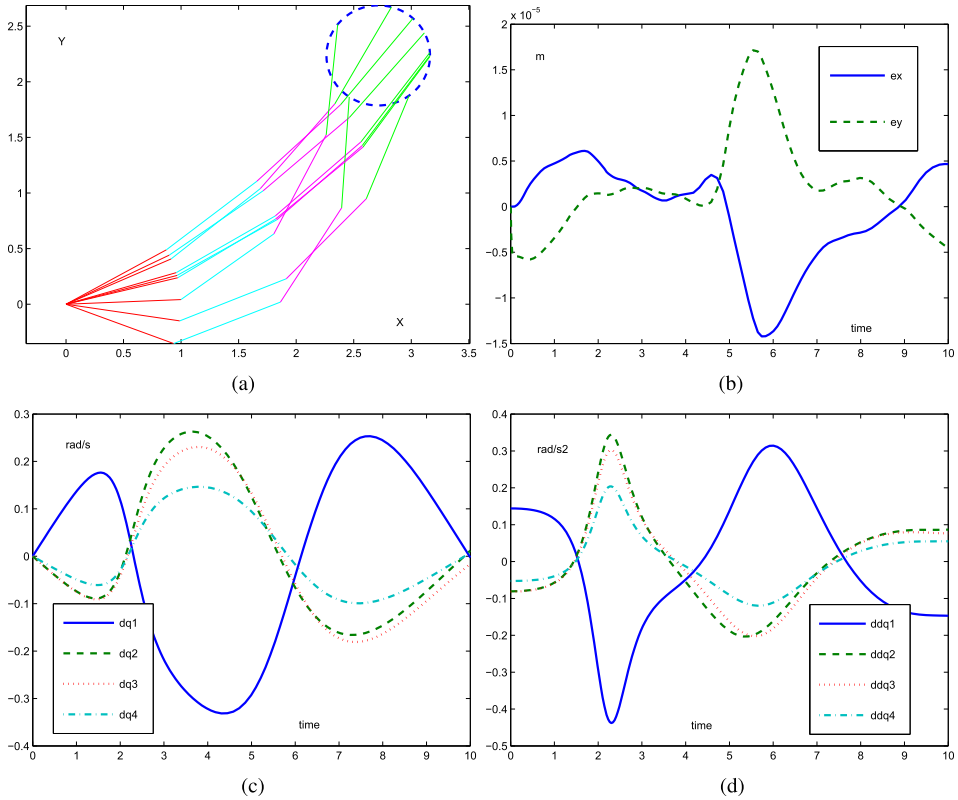

FIGURE 3. The four-link robot manipulator tracks a circular path by using the proposed FPBM scheme (13) with $\alpha = 0.6$, $k_1 = k_2 = 1$ and $W = \text{diag}\{1, 4, 9, 16\}$. (a) Motion trajectories. (b) End-effector tracking errors. (c) Profiles of joint velocity $\dot{q}$. (d) Profiles of joint acceleration $\ddot{q}$.

which is the FPBM scheme (13) proposed in this paper for the kinematic control of redundant robot manipulators. The proof is thus completed. □

The proposed FPBM scheme (13) is changed to the feedback-added MAN scheme as $\alpha = 0$, and is changed to WMVN scheme as $\alpha = 1$. When $\alpha \in (0, 1)$, the proposed scheme processes simultaneously the MAN and WMVN characteristics. By selecting a suitable α, the proposed FPBM scheme (13) can remedy the phenomena of (relatively) high joint velocity and joint acceleration, generate a near-zero final joint velocity, and guarantee a nondivergent end-effector tracking error.

IV. SIMULATION VERIFICATION

In this section, simulation results based on a four-link robot manipulator [21] with different tracking examples are performed to verify the effectiveness of the proposed FPBM scheme (13).

A. CIRCULAR PATH TRACKING EXAMPLE

In this example, the proposed FPBM scheme (13) is applied to the four-link robot manipulator when its end-effector tracks a circle with radius of 0.25 m. In addition, the task duration is $T = 10$ s and the initial joint state is $q(0) = [\pi/15, \pi/15, \pi/12, \pi/12]^{\mathrm{T}}$ rad. For comparison, the MAN scheme (8) is simulated here. The simulation results by using (8) and (13) are presented in Figs. 1–3 and Tables 1–3.

Fig. 1 illustrates the results by using the MAN scheme (8). In Fig. 1(a) and (b), the end-effector of the robot manipulator tracks effectively the desired circular path, where the maximal tracking error is about 8.0×10^{-5} m. However, Fig. 1(b) shows that there exist the divergence phenomenon in the end-effector tracking error. In addition, Fig. 1(c) and (d) show that some value of joint velocity $\dot{q}$ and joint acceleration $\ddot{q}$ appear to be (relatively) large. Furthermore, Fig. 1(c) shows that some final joint velocities are not zero. The detailed data are $\dot{q}(10) = [0.408275, -0.430472, -0.174470, 0.000112]^{\mathrm{T}}$ rad/s. Evidently, the final joint velocities are too large. Thus, the MAN scheme (8) is less applicable in terms of the divergent tracking error and the non-zero joint velocity at the end of motion.

Fig. 2 presents the results by using the proposed FPBM scheme (13) with $\alpha = 0.6$, $k_1 = k_2 = 1$ and $W = \text{diag}\{1, 2, 3, 4\}$. In Fig. 2(a) and (b), the robot manipulator successfully finishes the circular path tracking task, where the maximal tracking error is about 1.5×10^{-5} m. By comparing Fig. 1(b) and Fig. 2(b), we find that the maximal error via the proposed FPBM scheme (13) is about six times smaller than that via the MAN scheme (8). In addition, no divergence phenomenon exists in the tracking error, thereby indicating the advantage of (13) by

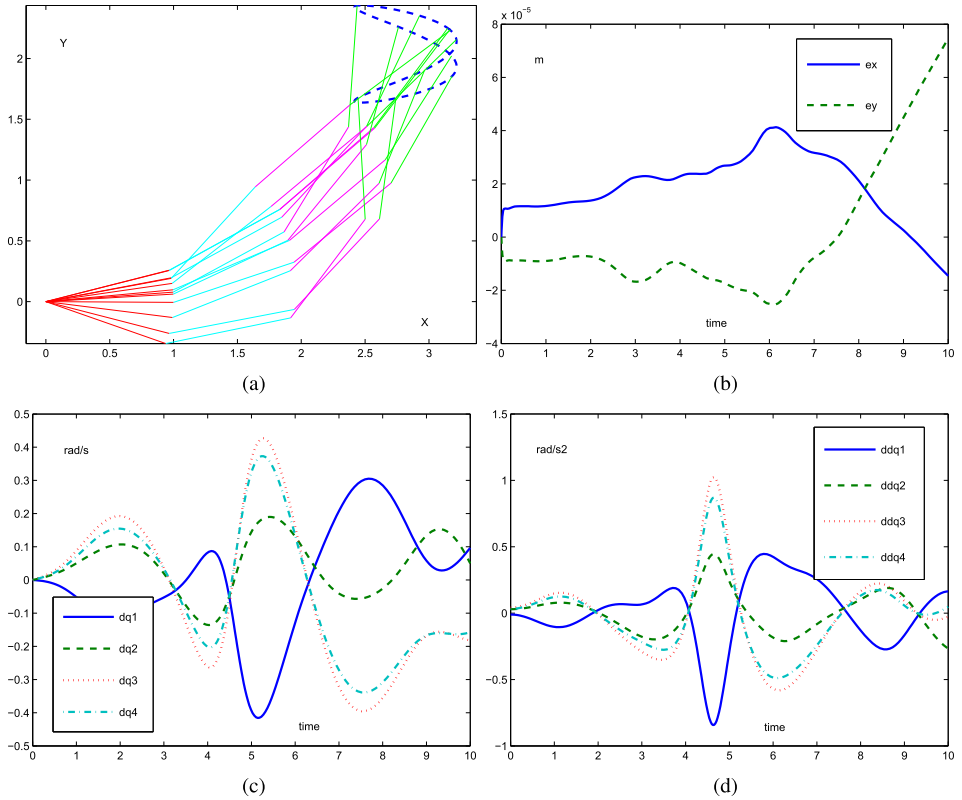

FIGURE 4. The four-link robot manipulator tracks a Lissajous-figure path by using the MAN scheme (8). (a) Motion trajectories. (b) End-effector tracking errors. (c) Profiles of joint velocity $\dot{q}$. (d) Profiles of joint acceleration $\ddot{q}$.

TABLE 1. End-effector tracking errors (m) and final joint velocities (rad/s) when the four-link robot manipulator tracks the circular path by using the proposed FPBM scheme (13) with $k_1 = k_2 = 1$, $W = \text{diag}\{1, 2, 3, 4\}$ and different α.

α	error	$\dot{q}_1(10)$	$\dot{q}_2(10)$	$\dot{q}_3(10)$	$\dot{q}_4(10)$
0.4	$\leqslant 1.960 \times 10^{-5}$	-0.010657	0.062907	-0.052505	-0.042819
0.5	$\leqslant 1.395 \times 10^{-5}$	-0.011669	0.045533	-0.034669	-0.022324
0.6	$\leqslant 1.324 \times 10^{-5}$	-0.009308	0.030958	-0.023297	-0.010275
0.7	$\leqslant 1.517 \times 10^{-5}$	-0.006264	0.019461	-0.015298	-0.003447
0.8	$\leqslant 1.582 \times 10^{-5}$	-0.003512	0.010725	-0.009191	-0.000084

introducing the feedback. Fig. 2(c) and (d) shows that the values of $\dot{q}$ and $\ddot{q}$ are relatively small, as compared with those shown in Fig. 1(c) and (d). Fig. 2(c) also shows that the final joint velocities are near zero. The detailed data are $\dot{q}(10) = [-0.009308, 0.030958, -0.023297, -0.010275]^{\mathrm{T}}$ rad/s (being acceptable for applications). Evidently, these simulation results verify the effectiveness and superiority of the proposed FPBM scheme (13) over the MAN scheme (8). More comparative simulation results are presented in the Appendix.

By changing the values of α (i.e., $\alpha = 0.4, 0.5, 0.6, 0.7$ and 0.8), the proposed FPBM scheme (13) with $k_1 = k_2 = 1$ and $W = \text{diag}\{1, 2, 3, 4\}$ is simulated, and the related data are given in Table 1. This table shows that the end-effector tracking errors via (13) are in the order 10^{-5} m. Table 1 also shows that the joint velocities at $t = 10$ s (i.e. the final joint velocities) are near zero. Evidently, these results verify that the proposed FPBM scheme (13) is effective on the kinematic control of the four-link robot manipulator. Furthermore, the data shown in Table 1 indicate the flexibility of (13); that is, different α can be selected for the proposed FPBM scheme (13) to achieve a suitable performance

TABLE 2. End-effector tracking errors (m) when the robot manipulator tracks the circular path by using the proposed scheme (13) with $\alpha = 0.6$, $k_1 = k_2 = 1$ and different W.

W	error
$W_1 = \text{diag}\{2, 2, 4, 4\}$	$\leqslant 1.262 \times 10^{-5}$
$W_2 = \text{diag}\{4, 4, 9, 9\}$	$\leqslant 1.332 \times 10^{-5}$
$W_3 = \text{diag}\{9, 9, 16, 16\}$	$\leqslant 1.214 \times 10^{-5}$
$W_4 = \text{diag}\{2, 4, 6, 8\}$	$\leqslant 1.324 \times 10^{-5}$
$W_5 = \text{diag}\{10, 12, 14, 16\}$	$\leqslant 1.355 \times 10^{-5}$
$W_6 = \text{diag}\{16, 16, 16, 16\}$	$\leqslant 1.411 \times 10^{-5}$

With $\alpha = 0.6$ and $k_1 = k_2 = 1$ fixed, by changing W to $\text{diag}\{1, 4, 9, 16\}$, the proposed FPBM scheme (13) is simulated, and the related results are presented

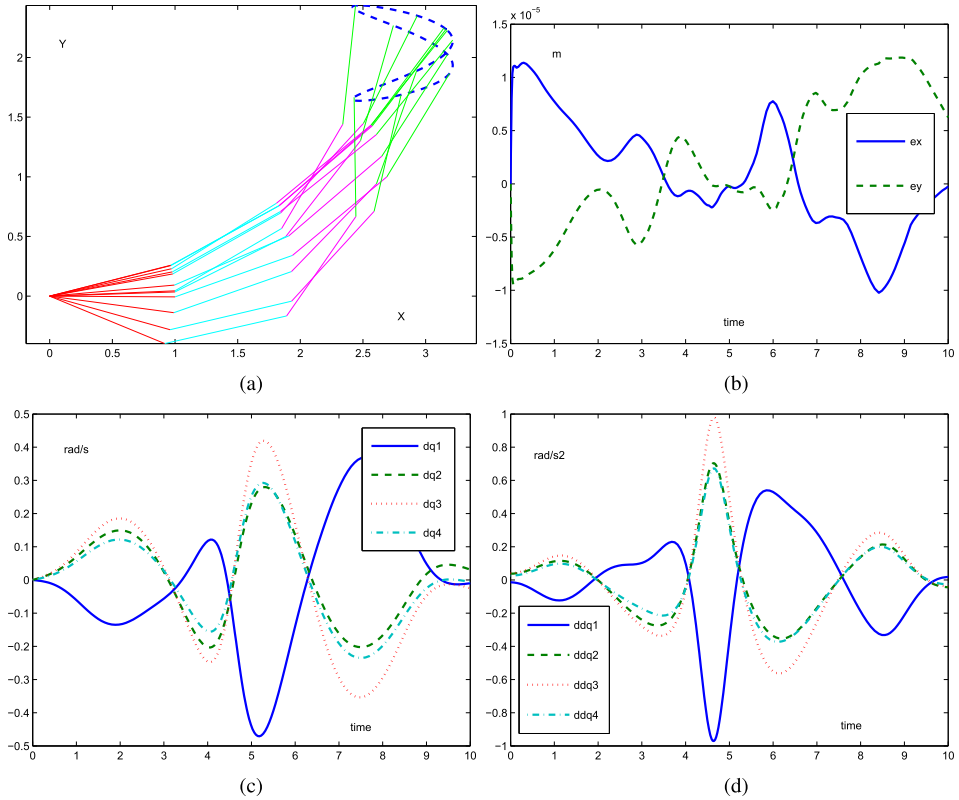

FIGURE 5. The four-link robot manipulator tracks a Lissajous-figure path by using the proposed FPBM scheme (13) with $\alpha = 0.6$, $k_1 = k_2 = 1$ and $W = \text{diag}\{2, 4, 6, 8\}$. (a) Motion trajectories. (b) End-effector tracking errors. (c) Profiles of joint velocity $\dot{q}$. (d) Profiles of joint acceleration $\ddot{q}$.

in Fig. 3. In Fig. 3(a) and (b), the circular path tracking task is effectively fulfilled by the robot manipulator with the maximal tracking error being about 2.0×10^{-5} m. In addition, there does not exist the divergence issue in the tracking error, as shown in Fig. 3(b). In Fig. 3(c) and (d), the values of $\dot{q}$ and $\ddot{q}$ are relatively small, and the final velocities are near zero (with the detailed data being $\dot{q}(10) = [-0.002759, 0.011884, -0.015928, 0.007059]^{\mathrm{T}}$ rad/s). These simulation results verify again the effectiveness of the proposed FPBM scheme (13).

By selecting more W [i.e., $W_1 = \text{diag}\{2, 2, 4, 4\}$, $W_2 = \text{diag}\{4, 4, 9, 9\}$, $W_3 = \text{diag}\{9, 9, 16, 16\}$, $W_4 = \text{diag}\{2, 4, 6, 8\}$, $W_5 = \text{diag}\{10, 12, 14, 16\}$, and $W_6 = \text{diag}\{16, 16, 16, 16\}$], the proposed FPBM scheme (13) with $\alpha = 0.6$ and $k_1 = k_2 = 1$ is simulated, and the related data are given in Tables 2 and 3. In Table 2, by using (13) with different W, the end-effector tracking errors are still small enough and are in the order 10^{-5} m. In Table 3, all the joint velocities at $t = 10$ s are near zero. Evidently, these results verify again that the proposed FPBM scheme (13) is effective on the four-link robot manipulator. Note that, for each selection of W, (13) is tested by changing the values of α. The related results, which are similar to those in Table 1 and are thus omitted here, also show that the maximal end-effector tracking error is small and does not introduce the divergence phenomenon. In addition, the $\dot{q}$ and $\ddot{q}$ values are relatively small, and the final velocities are near zero. Thus, the effective and flexible performance of the proposed FPBM scheme (13) is indicated once again.

TABLE 3. Final joint velocities (rad/s) when the robot manipulator tracks the circular path by using the proposed scheme (13) with $\alpha = 0.6$, $k_1 = k_2 = 1$ and different W.

W	$\dot{q}_1(10)$	$\dot{q}_2(10)$	$\dot{q}_3(10)$	$\dot{q}_4(10)$
W_1	-0.010465	0.033695	-0.020044	-0.020581
W_2	-0.009610	0.029546	-0.017411	-0.016655
W_3	-0.011103	0.037813	-0.022933	-0.024740
W_4	-0.009308	0.030958	-0.023297	-0.010276
W_5	-0.011563	0.046926	-0.032825	-0.030629
W_6	-0.010252	0.055416	-0.039821	-0.047208

In summary, the above results (i.e., Figs. 1–3 and Tables 1–3) have verified the effectiveness of the proposed FPBM scheme (13), as compared with the MAN scheme (8).

B. LISSAJOUS-FIGURE PATH TRACKING EXAMPLE

In this example, the proposed FPBM scheme (13) is simulated the four-link robot manipulator when its end-effector tracks a Lissajous-figure path. The task duration and the initial joint state are the same as before. The simulation results are presented in Figs. 4–6.

Fig. 4 shows the results by using the MAN scheme (8). As shown in Fig. 4, although the robot's end-effector

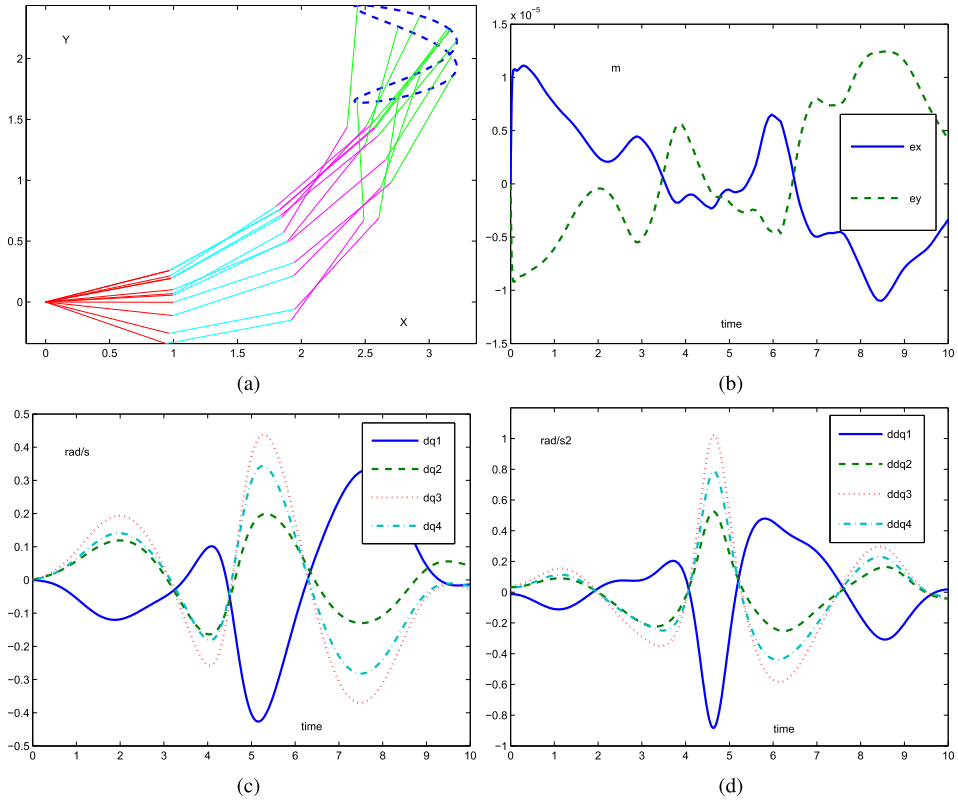

FIGURE 6. The four-link robot manipulator tracks a Lissajous-figure path by using the proposed FPBM scheme (13) with $\alpha = 0.6$, $k_1 = k_2 = 1$ and $W = \text{diag}\{10, 12, 14, 16\}$. (a) Motion trajectories. (b) End-effector tracking errors. (c) Profiles of joint velocity $\dot{q}$. (d) Profiles of joint acceleration $\ddot{q}$.

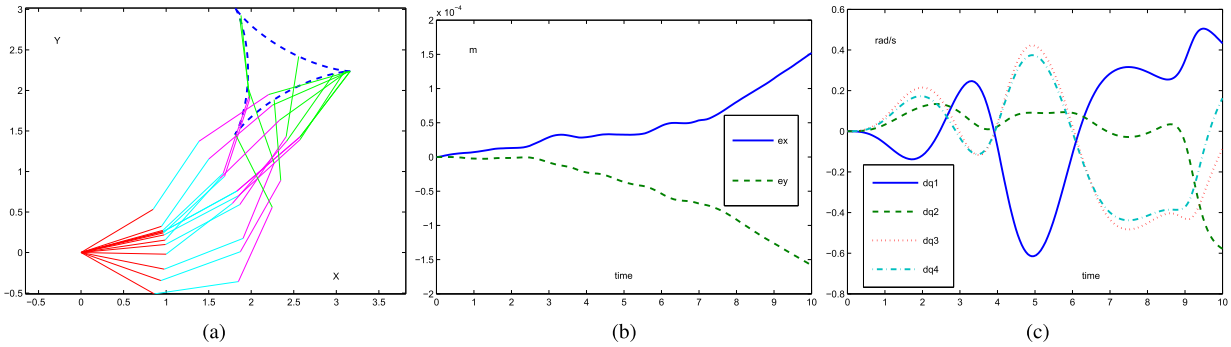

FIGURE 7. The four-link robot manipulator tracks a tricuspid path by using the MAN scheme (8). (a) Motion trajectories. (b) End-effector tracking errors. (c) Profiles of joint velocity $\dot{q}$.

tracks effectively the desired path, some issues are still encountered. That is, the divergence phenomenon exists in the end-effector tracking error, and some final joint velocities are not zero (with the detailed data being $\dot{q}(10) = [0.096595, 0.049759, -0.182648, -0.157152]^{\mathrm{T}}$ rad/s). Obviously, these results indicate again that the MAN scheme (8) is less applicable in robotic practice.

Fig. 5 presents the results by using the proposed FPBM scheme (13) with $\alpha = 0.6$, $k_1 = k_2 = 1$ and $W = \text{diag}\{2, 4, 6, 8\}$. In Fig. 5(a) and (b), the robot's end-effector tracks the Lissajous-figure path successfully with a small and nondivergent tracking error. In Fig. 5(c) and (d), the joint velocity and joint acceleration values are relatively small, and the final joint velocities are $\dot{q}(10) = [-0.009833, 0.031417, -0.024939, 0.006216]^{\mathrm{T}}$ rad/s (being near zero). Evidently, comparing Fig. 5 with Fig. 4 verifies the effectiveness and superiority of the proposed FPBM scheme (13) over the MAN scheme (8). More comparative simulation results are presented in the Appendix. Fig. 6 shows the results of (13) by changing W to $\text{diag}\{10, 12, 14, 16\}$ from which the observation is similar to that from Fig. 5. Evidently, Fig. 6 indicates again that the proposed FPBM scheme (13)

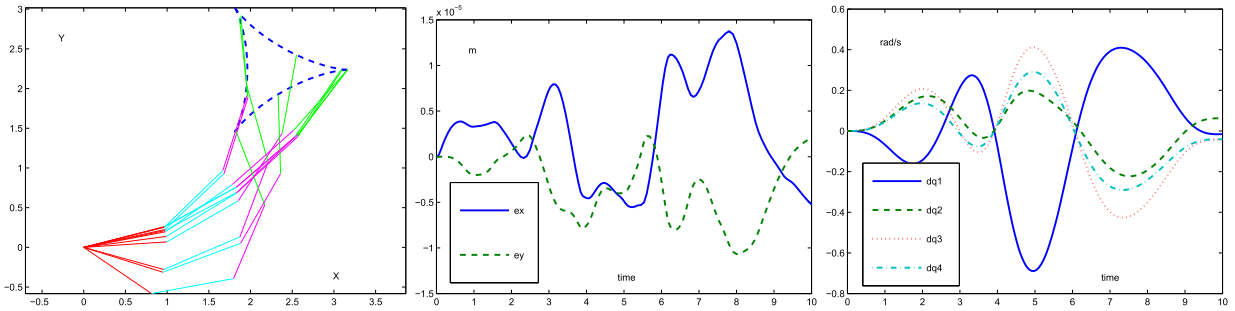

(a) (b) (c)

FIGURE 8. The four-link robot manipulator tracks a tricuspid path by using the proposed FPBM scheme (13) with $\alpha = 0.6$, $k_1 = k_2 = 1$ and $W = \text{diag}\{2, 4, 6, 8\}$. (a) Motion trajectories. (b) End-effector tracking errors. (c) Profiles of joint velocity $\dot{q}$.

is effective on the kinematic control of the four-link robot manipulator.

Remark 1: The weighting factor α in the proposed FPBM scheme (13) scales the combined effect of WMVN and MAN solutions. Different α in (0, 1) can be selected for different requirements. For example, if a solution where WMVN has more effect in comparison with MAN is needed, then α can be selected as a larger one. By selecting different α for (13) in the simulations, it can be concluded that α in (13) can be determined by the requirements of an acceptable tracking error and the $\dot{q}$ and $\ddot{q}$ solutions stability.

Remark 2: Different selections of W also lead to different effects of the proposed FPBM scheme (13). Using $W = \text{diag}\{w_1, w_2, \cdots, w_n\} \in R^{n\times n}$ can be the common one in (13). By following the simulation results in Figs. 2–6 and Tables 1–3), it can be concluded that the element in W could be selected as a relatively large value to achieve a small end-effector tracking error and a near-zero final joint velocity. More studies on how to select W can be the future research direction.

V. CONCLUSION

In this paper, the new FPBM scheme (13) has been proposed and studied for the kinematic control of redundant robot manipulators. Such a scheme has been designed based on the combination of the WMVN and MAN schemes and the introduction of the feedback. Based on a four-link robot manipulator with different illustrative examples, simulation results have been presented to verify the effectiveness of the proposed FPBM scheme (13) on robotic redundancy resolution. That is, the proposed scheme can prevent the occurrence of high velocity and acceleration, generate a near-zero final velocity, and guarantee a nondivergent end-effector tracking error.

The proposed FPBM scheme (13) is the first pseudoinverse-type scheme that combines the MAN and WMVN solutions. This is significant as it shows potentials on the design of more different balanced minimization schemes for redundant robot manipulators. By following this paper, the proposed FPBM scheme (13) is expected to applied to a practical robot manipulator, as one of the future research directions.

APPENDIX

In this appendix, more comparative results of the MAN scheme (8) and the proposed FPBM scheme (13) are presented, where the four-link robot manipulator is expected to track a tricuspid path.

Specifically, by using the MAN scheme (8), Fig. 7 shows the related results. This figure indicates that (8) is less applicable in terms of the divergence phenomenon in the end-effector tracking error and the not zero problem in the final joint velocity. By contrast, Fig. 8 presents the results by using the proposed FPBM scheme (13) with $\alpha = 0.6$, $k_1 = k_2 = 1$ and $W = \text{diag}\{2, 4, 6, 8\}$. As observed from Fig. 8, the robot's end-effector matches the tricuspid path successfully with a small and nondivergent error. In addition, the joint velocities are relatively small and the final joint velocities are near zero (with the detailed data being $\dot{q}(10) = [-0.015436, 0.063234, -0.042985, -0.040725]^{\mathrm{T}}$ rad/s). This means that the undesired issues that exist in Fig. 7 are not encountered in Fig. 8. Thus, these comparative results the effective and superior properties of the proposed FPBM scheme (13) over the MAN scheme (8).

REFERENCES

[1] B. Siciliano and O. Khatib, *Springer Handbook of Robotics*. Heidelberg, Germany: Springer-Verlag, 2008.
[2] B. Siciliano, L. Sciavicco, L. Villani, and G. Oriolo, *Robotics: Modelling, Planning and Control*. London, U.K.: Springer-Verlag, 2009.
[3] Y. Zhang and L. Jin, *Robot Manipulator Redundancy Resolution*. Hoboken, NJ, USA: Wiley, 2017.
[4] A. Motahari, H. Zohoor, and M. H. Korayem, "A new motion planning method for discretely actuated hyper-redundant manipulators," *Robotica*, vol. 35, no. 1, pp. 101–118, 2017.
[5] D. Guo, K. Li, and B. Liao, "Bi-criteria minimization with MWVN–INAM type for motion planning and control of redundant robot manipulators," *Robotica*, vol. 36, no. 5, pp. 655–675, 2018.
[6] L. Jin, S. Li, J. Yu, and J. He, "Robot manipulator control using neural networks: A survey," *Neurocomputing*, vol. 285, pp. 23–34, Apr. 2018.
[7] Z. Zhang, Y. Lu, L. Zheng, S. Li, Z. Yu, and Y. Li, "A new varying-parameter convergent-differential neural-network for solving time-varying convex QP problem constrained by linear-equality," *IEEE Trans. Autom. Control*, vol. 63, no. 12, pp. 4110–4125, Dec. 2018. doi: 10.1109/TAC.2018.2810039.
[8] Z. Zhang *et al.*, "A varying-parameter convergent-differential neural network for solving joint-angular-drift problems of redundant robot manipulators," *IEEE/ASME Trans. Mechatronics*, vol. 23, no. 2, pp. 679–689, Apr. 2018.

[9] L. Xiao, Y. Zhang, B. Liao, Z. Zhang, L. Ding, and L. Jin, "A velocity-level bi-criteria optimization scheme for coordinated path tracking of dual robot manipulators using recurrent neural network," *Frontiers Neurorobot.*, vol. 11, no. 9, p. 47, 2017.

[10] Y. Chen and C. Shen, "Performance analysis of smartphone-sensor behavior for human activity recognition," *IEEE Access*, vol. 5, pp. 3095–3110, 2017.

[11] G. Sun, L. Wu, Z. Kuang, Z. Ma, and J. Liu, "Practical tracking control of linear motor via fractional-order sliding mode," *Automatica*, vol. 94, pp. 221–235, Aug. 2018.

[12] Y. Zhao, Y. Shen, A. Bernard, C. Cachard, and H. Liebgott, "Evaluation and comparison of current biopsy needle localization and tracking methods using 3D ultrasound," *Ultrasonics*, vol. 73, pp. 206–220, Jan. 2017.

[13] Y. Zhao, J. Wang, F. Yan, and Y. Shen, "Adaptive sliding mode fault-tolerant control for type-2 fuzzy systems with distributed delays," *Inf. Sci.*, vol. 473, pp. 227–238, Jan. 2019.

[14] A. S. Deo and I. D. Walker, "Minimum effort inverse kinematics for redundant manipulators," *IEEE Trans. Robot. Autom.*, vol. 13, no. 5, pp. 767–775, Oct. 1997.

[15] I. A. Gravagne and I. D. Walker, "On the structure of minimum effort solutions with application to kinematic redundancy resolution," *IEEE Trans. Robot. Autom.*, vol. 16, no. 6, pp. 855–863, Dec. 2000.

[16] L. Jin, S. Li, L. Xiao, R. Lu, and B. Liao, "Cooperative motion generation in a distributed network of redundant robot manipulators with noises," *IEEE Trans. Syst., Man, Cybern., Syst.*, vol. 48, no. 10, pp. 1715–1724, Oct. 2018.

[17] M. G. Marcos, J. A. T. Machado, and T.-P. Azevedo-Perdicoúlis, "A multi-objective approach for the motion planning of redundant manipulators," *Appl. Soft Comput.*, vol. 12, no. 2, pp. 589–599, 2012.

[18] Y. Zhang, S. Chen, S. Li, and Z. Zhang, "Adaptive projection neural network for kinematic control of redundant manipulators with unknown physical parameters," *IEEE Trans. Ind. Electron.*, vol. 65, no. 6, pp. 4909–4920, Jun. 2018.

[19] F. Flacco, A. De Luca, and O. Khatib, "Motion control of redundant robots under joint constraints: Saturation in the null space," in *Proc. IEEE Int. Conf. Robot. Autom*. May 2012, pp. 285–292.

[20] G. Sun, Z. Ma, and J. Yu, "Discrete-time fractional order terminal sliding mode tracking control for linear motor," *IEEE Trans. Ind. Electron.*, vol. 65, no. 4, pp. 3386–3394, Apr. 2018.

[21] B. Liao and W. Liu, "Pseudoinverse-type bi-criteria minimization scheme for redundancy resolution of robot manipulators," *Robotica*, vol. 33, no. 10, pp. 2100–2113, Dec. 2015.

[22] F. Flacco and A. De Luca, "Discrete-time redundancy resolution at the velocity level with acceleration/torque optimization properties," *Robot. Auto. Syst.*, vol. 70, pp. 191–201, Aug. 2015.

[23] F. Flacco, A. De Luca, and O. Khatib, "Control of redundant robots under hard joint constraints: Saturation in the null space," *IEEE Trans. Robot.*, vol. 31, no. 3, pp. 637–654, Jun. 2015.

[24] D. Guo, F. Xu, and L. Yan, "New pseudoinverse-based path-planning scheme with PID characteristic for redundant robot manipulators in the presence of noise," *IEEE Trans. Control Syst. Technol.*, vol. 26, no. 6, pp. 2008–2019, Nov. 2018. doi: 10.1109/TCST.2017.2756029.

[25] J. Liu, Y. Gao, X. Su, M. Wack, and L. Wu, "Disturbance-observer-based control for air management of PEM fuel cell systems via sliding mode technique," *IEEE Trans. Control Syst. Technol.*, to be published. doi: 10.1109/TCST.2018.2802467.

[26] J. Liu, H. An, Y. Gao, C. Wang, and L. Wu, "Adaptive control of hypersonic flight vehicles with limited angle-of-attack," *IEEE/ASME Trans. Mechatronics*, vol. 23, no. 2, pp. 883–894, Apr. 2018.

[27] D. Guo, F. Xu, L. Yan, Z. Nie, and H. Shao, "A new noise-tolerant obstacle avoidance scheme for motion planning of redundant robot manipulators," *Frontiers Neurorobot.*, vol. 12, pp. 51–63, Aug. 2018.

[28] K. A. O'Neil, "Divergence of linear acceleration-based redundancy resolution schemes," *IEEE Trans. Robot. Autom.*, vol. 18, no. 4, pp. 625–631, Aug. 2002.

[29] J. Liu, Y. Yin, W. Luo, S. Vazquez, L. G. Franquelo, and L. Wu, "Sliding mode control of a three-phase AC/DC voltage source converter under unknown load conditions: Industry applications," *IEEE Trans. Syst., Man, Cybern., Syst.*, vol. 48, no. 10, pp. 1771–1780, Oct. 2018.

[30] C. Shen, Y. Li, Y. Chen, X. Guan, and R. Maxion, "Performance analysis of multi-motion sensor behavior for active smartphone authentication," *IEEE Trans. Inf. Forensics Security*, vol. 13, no. 1, pp. 48–62, Jan. 2018.

[31] Y. Gao, J. Liu, G. Sun, M. Liu, and L. Wu, "Fault deviation estimation and integral sliding mode control design for Lipschitz nonlinear systems," *Syst. Control Lett.*, vol. 123, pp. 8–15, Jan. 2019.

[32] C. A. Klein and C.-H. Huang, "Review of pseudoinverse control for use with kinematically redundant manipulators," *IEEE Trans. Syst., Man, Cybern.*, vol. SMC-13, no. 2, pp. 245–250, Mar./Apr. 1983.

[33] K. Kazerounian and Z. Wang, "Global versus local optimization in redundancy resolution of robotic manipulators," *Int. J. Robot. Res.*, vol. 7, no. 5, pp. 3–12, 1988.

[34] A. De Luca, L. Lanari, and G. Oriolo, "Control of redundant robots on cyclic trajectories," in *Proc. IEEE Int. Conf. Robot. Autom.*, May 1992, pp. 500–506.

[35] Z. Kemény, "Redundancy resolution in robots using parameterization through null space," *IEEE Trans. Ind. Electron.*, vol. 50, no. 4, pp. 777–783, Aug. 2003.

[36] K. Tchoń, "Optimal extended jacobian inverse kinematics algorithms for robotic manipulators," *IEEE Trans. Robot.*, vol. 24, no. 6, pp. 1440–1445, Dec. 2008.

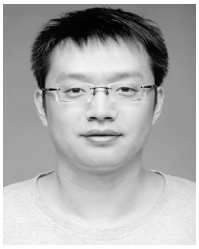

ZHENHUAN WANG received the B.S. and M.S. degrees in automation from the Harbin Institute of Technology, China, in 2006 and 2008, respectively, and the Ph.D. degree in control science and engineering from the Space Control and Inertial Technology Research Center, Harbin Institute of Technology, in 2013. He has been an Assistant Professor with the Space Control and Inertial Technology Research Center, Harbin Institute of Technology, since 2013, where he is currently an Associate Professor. His research interests include guidance, navigation, and control.

BOYANG WANG was born in Hunan, China, in 1998. He is currently pursuing the bachelor's degree in automation engineering with the School of Astronautics, Harbin Institute of Technology, China. His research interests include control and artificial intelligence.

LINGJIE XU received the B.S. degree in automation from the Harbin Institute of Technology, China, in 2018, where he is currently pursuing the M.S. degree. His research interest includes power electronics.

QINYU XIE was born in 1998. He is currently pursuing the bachelor's degree in automation with the School of Astronautics, Harbin Institute of Technology, China. His research interest includes control.